Upscaling of Land Surface Parameters through Inverse SVAT-Modeling

Joseph Intsiful

Centre for Development Research (ZEF), University of Bonn, and

Institute for Meteorology and Climate Research (IMK-IFU),

Forschungszentrum Karlsruhe, Kreuzeckbahnstrasse 19,

D-82467 Garmisch-Partenkirchen

Email: joseph.intsiful@imk.fzk.de

Phone: ++49 (0)8821 183 214

1. OVERVIEW

1.1 Motivation

Ongoing intensification of agriculture in West Africa has led to a change in surface and subsurface characteristics, which directly affect evapotranspiration rates. If these changed evapotranspiration rates in turn affect regional precipitation patterns, rainfed and irrigated agriculture in West Africa may face changed boundary conditions because of complex feedback mechanisms between the surface and atmosphere. The investigation of these feedback effects requires the application of regional climate models that account for soil and vegetation state through SVAT schemes.

Regional climate models use land use data in resolutions of 10-250 km because of the limitation of computing resources required for fine resolution runs over the domain of interest. However, information on land surface parameters is usually available at much finer resolution. It is a fundamental and not yet satisfactorily solved problem in hydrological research how subgrid scale variability can be accounted for at coarse resolutions.

We therefore investigate into the possibility to derive “effective” parameters on grid scale (in dependence of mean and standard deviation at subgrid scale) that yield approximately the same surface heat fluxes as the corresponding aggregated fluxes on the finer scale.

1.2 Objectives

This work aims to derive effective soil and vegetation parameters accounting for subgrid scale variability in SVAT models and regional climate models.

Specific objectives are

- To undertake sensitivity analysis of SVAT-model parameters with respect to latent and sensible heat fluxes to identify sensitive SVAT parameters
- To develop a parameter estimation environment for SVAT models (stand alone and full 3-D).
- To investigate into suited objective functions for the estimation of selected soil and vegetation parameters.
- To derive upscaling laws, lookup table (LUT) respectively, for soil and vegetation parameters in SVAT models, with particular emphasis on the Volta basin
- To compare the developed method to existing aggregation/upscaling schemes
- To investigate differences between derived effective parameters for SVAT models in stand alone mode (1-D) and fully 3-D mode.
- To investigate into the uniqueness of the estimated parameters.

1.3 Achievements

The achievements so far are

- Development of an inverse-SVAT modeling algorithm for estimating effective land surface parameters.
- Identification of optimal objective functions and parameter bounds.
- Derivation of upscaling laws, allowing to scale distributed land surface parameters from the sub-grid scale to the grid-scale: 1) roughness length, 2) albedo, 3) emissivity, 4) minimum stomatal resistance, 5) plant insolation factor, 6) vapor pressure deficit factor, 7) leaf area index and 8) Clapp-Hornberger soil parameter “b”.
- Comparison of aggregation scheme to Hu et al. (1999) and Noilhan et al. (1996).
- Differences between stand alone version and 3-D version.

- Identification of indeterminate states of solution; recommendation for selection of initial parameter guesses.

1.4 Problem Definition

Given a distributed heterogeneous land surface (characterized by landsurface parameters of mean μ_p and standard deviation σ_p) at the sub-grid scale, can we find an effective parameter p_{eff} at the grid scale such that the relative change in output response (e.g. surface energy fluxes and moisture indicators) is less than 10% (scale invariant)?

If such an effective parameter p_{eff} exists, can we find a functional relation that maps the mean μ_p and standard deviation σ_p of the distributed landsurface parameters at the subgrid scale to their corresponding effective parameter p_{eff} at the gridscale?

1.5 Solution Strategy

The solution strategy is to upscale the land surface parameters at the fine scale to the coarse scale through inverse-SVAT modeling. This is based on the premise that, if we can find a parameter set (sub-optimal solution) that is within a close neighborhood of the true parameter set, we can optimally adjust the parameter set to converge to the true parameter set.

We therefore seek approximate solutions (sub-optimal) and then optimally upgrade the parameter set till the scale invariant condition is met.

To realize this, we couple an existing, validated public domain SVAT model to the nonlinear parameter estimation tool PEST; we use approximate solutions as initial parameter values for the parameter estimation process. We extend the setup to the full 3D mesoscale case by coupling MM5 (which includes the same SVAT model as lower boundary) to PEST and repeat the process.

2. MODELS AND METHODS

Accounting for sub-grid scale effects in climate modeling is crucial for accurate representation of surface energy fluxes and moisture indicators on the grid-scale. Existing SVAT-models do not adequately account for sub-grid scale effects in the type of land surfaces, in particular encountered in the Savannah-mosaic of the Volta basin. To this end, a numerical experimentation using inverse-SVAT modeling was set up to estimate optimal effective parameters which adequately yield scale invariant outputs for surface temperature, incoming solar radiation, Bowen ratio, evaporative fraction, sensible and latent heat fluxes. The tunable effective parameters of interest were:

1) Surface albedo (surface property)
2) Emissivity (surface property)
3) Roughness length (surface property)
4) Minimum stomatal resistance (plant property)
5) Plant insolation factor (plant property)
6) Leaf area index (plant property)
7) Vapor pressure deficit factor (plant property)
8) Clapp-Hornberger soil parameter “b” (soil property)

In this numerical experimentation, the *OSU LSM* (Ek & Mahrt, 1991, see Fig. 1) SVAT model was coupled to the nonlinear parameter estimation tool PEST (Doherty, 2002) which is able to iteratively adjust the SVAT parameters such that scale invariant outputs are achieved. The SVAT model is driven by 1998 observation forcing data (4 days subset, Jan. 1^{st}-4^{th}) from the NOAA measurement site in Champaign (Meyers & Ek, 1999) which is characterized by vegetation type “groundcover only” and soil type “silty loam”. A Monte Carlo random number generator was used to provide parameter inputs to the SVAT model. Initial parameter estimates were derived from approximate methods of Hu et al. (1999) and related methods were used to initialize the nonlinear parameter estimation process. To verify if our model is independent of atmospheric forcing, we undertook extended runs for 28 days and the results obtained does not differ significantly from the usual four days episode runs used in this exercise.

The experiment was extended to cover the full 3-D mesoscale meteorological model MM5 to account for the lateral interactions between adjacent grid cells. The MM5 runs are initialized and run with NCEP reanalysis data. We perform a one way nested approach for five domains of grid sizes 3x3 km^2 (10x10 gridpoints), 3x3 km^2 (55x49), 9x9 km^2 (121x67), 27x27 km^2 (61x61) and 81x81 km^2 (61x61) where the outer boundaries provide boundary conditions to drive the inner domain. Here, we choose an area in the Volta Basin (West Africa) for our investigations (4 days subset Dec. 2^{nd} -5^{th} 1998).

We derived upscaling laws that maps the mean and standard deviation of the distributed land surface parameters (roughness length, albedo, emissivity, minimum stomatal resistance, plant insolation factor, leaf area index, vapor pressure deficit factor and Clapp-Hornberger soil parameter “b”) at the sub-grid scale to the corresponding effective parameter at the grid-scale. We verified the performance of our model by comparing our results to that of Hu et al. (1999). At small subgrid-scale variability the two methods correspond well. However, at higher levels of heterogeneity our method shows less deviation from the optimal, aggregated solution.

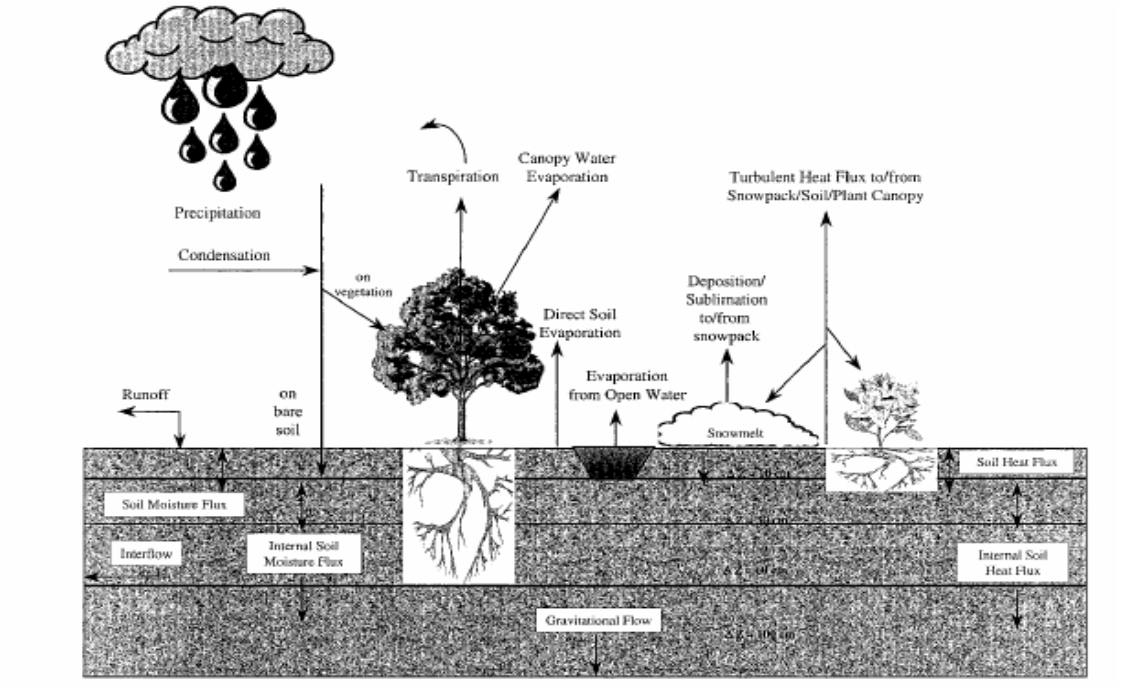

Fig. 1: A schematic representation of the OSU LSM in coupled MM5 model

Information on NOAH-SVAT (OSU-LSM, respectively) and PEST are given in the attached appendix. Since the SVAT model highly non-linearly transforms meteorological driving data (like wind, precipitation, radiation, temperature) into energy and water fluxes at the surface/subsurface, a nonlinear parameter estimation tool is required. PEST was our choice because it is based on the computationally efficient Marquardt-Levenberg algorithm. Moreover, it is a state of the art public domain tool which was successfully applied in many fields of geophysical research.

3.0 RESULTS

3.1 Theory of Developed Upscaling Method

The grid is subdivided into subgrids with parameters $p_i\,(i=1,..,n)$ characterized by a mean parameter p_{eff} and standard deviation σ_p (Fig. 2).

Fig. 2: Upscaling of land surface parameters

The subgrids in the fine resolution resolve the subgrid-scale variability at the gridscale. The coupled SVAT-PEST algorithm is used to estimate an effective parameter p_{eff} such that the aggregated output from the subgrid-scale $\sum_{i=1}^{n} a_i G_i = G(\mu_p, \sigma_p)$ (e.g. G: sensible heat flux) is almost equal to that at the grid scale $G(p_{eff})$ (Fig. 3).

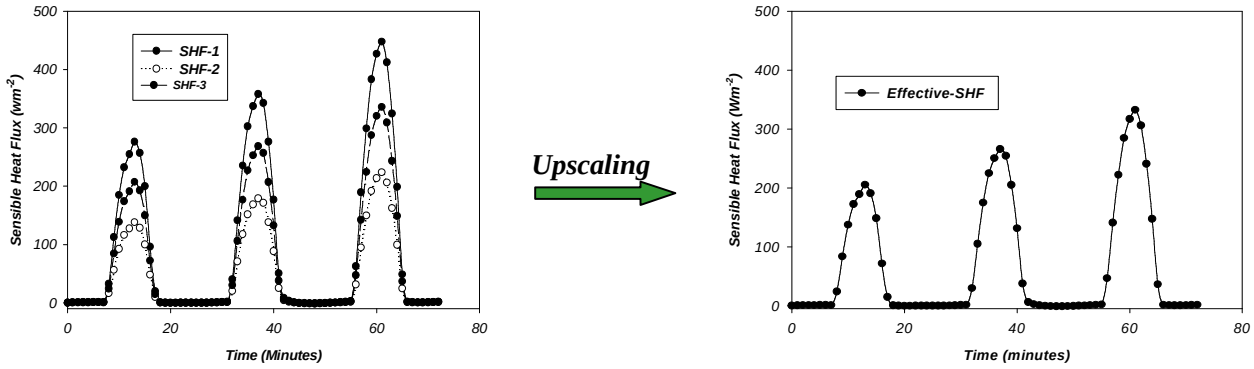

Subgrid scale fluxes: G_i Grid scale fluxes: G

Fig. 3: Aggregation of surface energy fluxes

The problem reduces to a root finding problem for p_{eff} , according to Eq. (1).:

$$\sum_{i=1}^{n} a_i G_i = G(\mu_p, \sigma_p) \overset{!}{\cong} G(p_{eff}) \qquad (1)$$

Fine Scale → *Coarse Scale*

We then proceed to derive an upscaling law $f(\mu_p, \sigma_p)$ which maps the mean $\hat{z}$ and standard deviation σ_p of the distributed parameters at the subgrid scale to their corresponding effective parameter p_{eff} at the grid scale. This upscaling law given by (1), is applied to sets of μ_p, σ_p as

$$p_{eff} = f(\mu_p, \sigma_p) \qquad (2)$$

To implement the solution strategy outlined above, a numerical experimentation is setup by coupling PEST to the OSU-LSM and the random number generator as shown in fig. 4.

The sequence of processes involved in the interaction between PEST, OSU-LSM and the random number generator is as follows:

1. Initially, a Monte Carlo simulation based on the normal distribution is used to generate synthetic parameters (representing a specific type of landsurface parameter e.g. RGL) that are used as inputs to PEST and OSU-LSM.

2. The synthetic parameters are used to estimate initial effective parameter estimates based on methods of Hu et al., (1999) and Noilhan et al., (1996) and then passed to PEST for initialization of the parameter estimation process. The synthetic parameters are also passed as input to the OSU LSM and the outputs aggregated as the weighted mean of individual output to obtain the experimental observation.

3. PEST then runs the OSU-LSM using the initial effective parameter estimates and compares the output with that of the experimental observation. If the difference is greater than some tolerance limit, PEST updates the parameter and the procedure is repeated till a termination criterion is reached.

The experiment is extended to the full 3-D climate scheme (MM5) to investigate the effect of lateral interactions of adjacent grids.

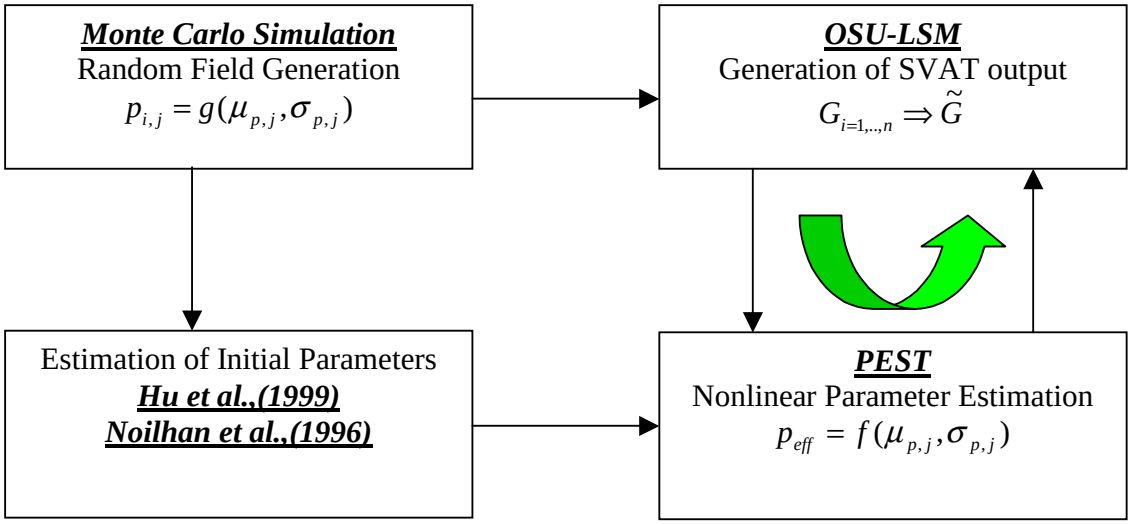

Fig. 4: Setup for the numerical experiment

3.2 Results for Coupled stand alone SVAT and PEST

a. Upscaling laws

To account for sub-grid scale effects, we derive upscaling laws that maps the mean and standard deviation of the distributed land surface parameters at the sub-grid scale to their corresponding effective parameter at the grid scale. Figs. 5 - 10 show the respective plots of the upscaling law for roughness length, minimal stomatal resistance

and the Clapp-Hornberger soil parameter b, the vapour pressure deficit and leaf area index.

In the case of the roughness length we found that both planar and parabolic fits (weakly parabolic) are suited to interpolate between obtained effective values. For upscaling laws of roughness length with fitting functions based on the latent heat fluxes and evaporative fraction, the parabolic law gives a better fit whereas for the sensible heat fluxes both linear and parabolic fits are suitable. We present plots for upscaling roughness length based on sensible heat fluxes as fitting function below.

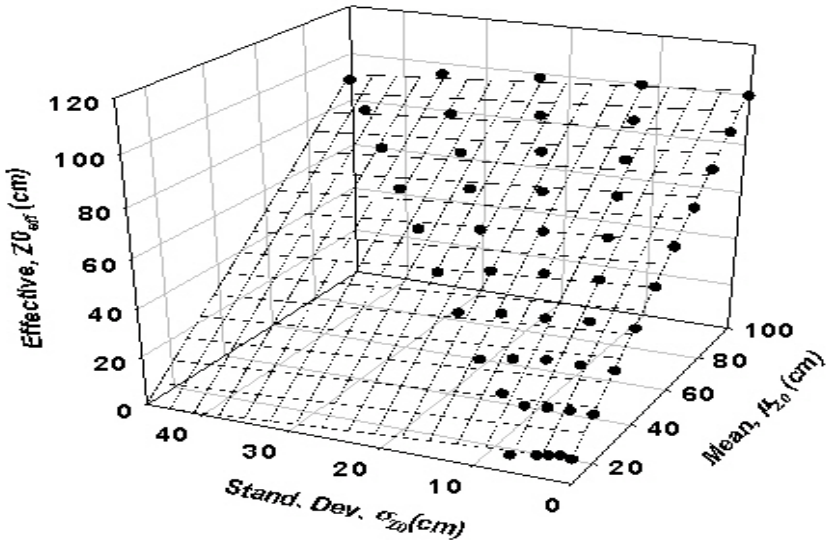

Fig. 5: Planar upscaling law for roughness length Z_0

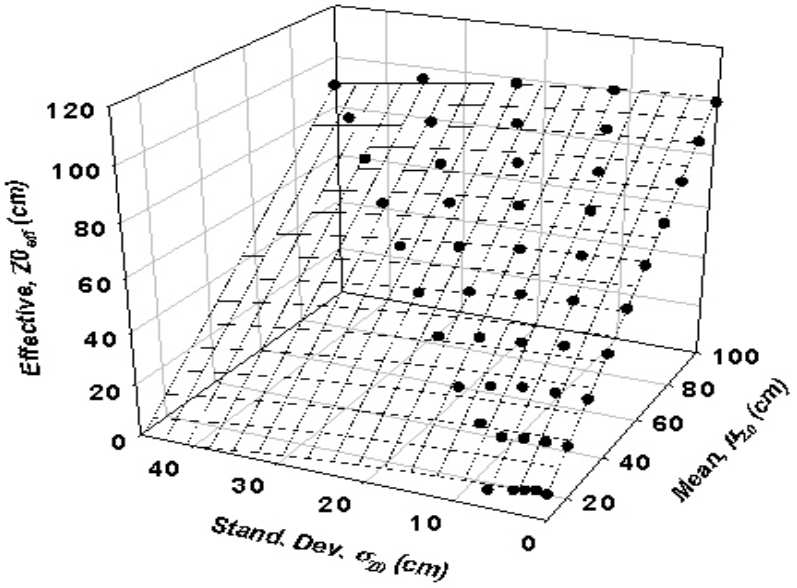

Fig. 6: Parabolic upscaling law for roughness length, Z_0

We found that parabolic fits are best suited to interpolate between the effective values of the Clapp-Hornberger soil parameter b and the minimum stomatal resistance. The measures of fit for these plots are given in table 3.

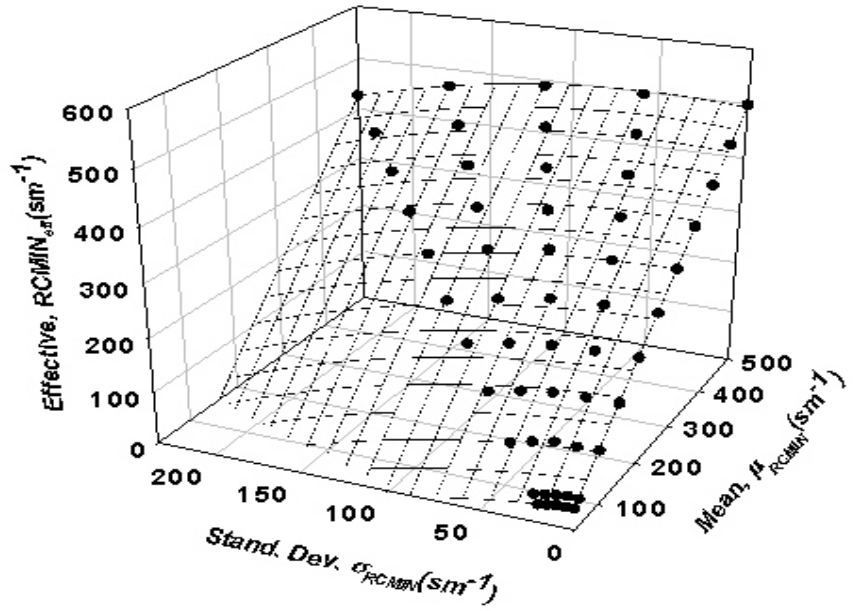

Fig. 7: Upscaling law for minimum stomatal resistance R_{cmin}

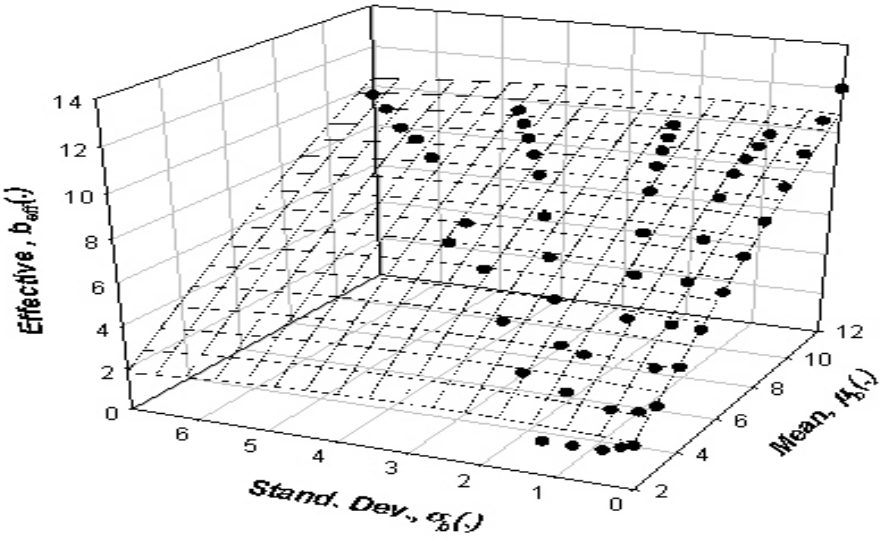

Fig. 8: Upscaling law for Clapp-Hornberger soil parameter, b

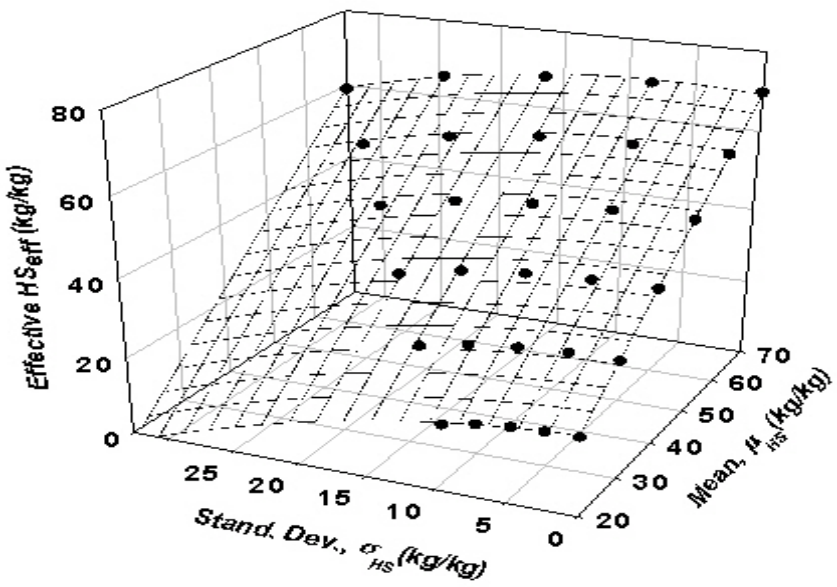

Fig. 9**:** Upscaling law for vapour pressure deficit factor HS

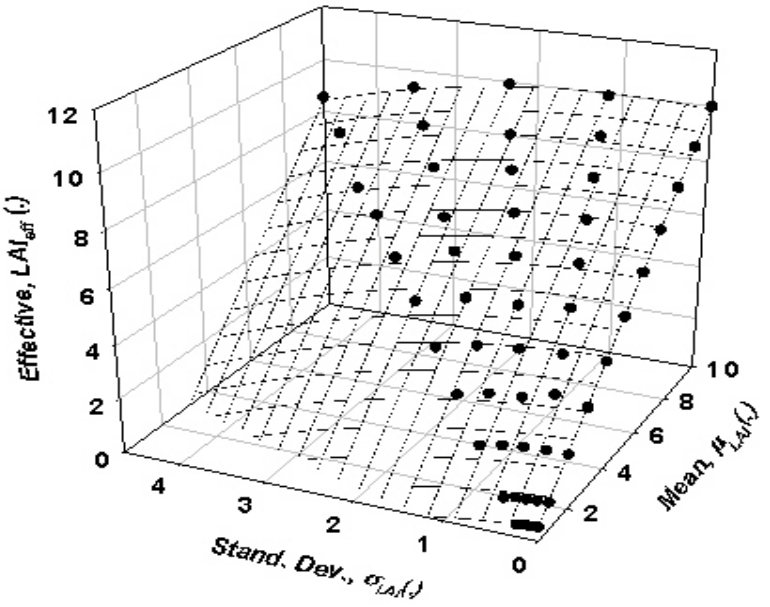

Fig. 10**:** Upscaling law for leaf area index, LAI

Table 1: Upscaling laws for OSU-PEST runs

Parameter	Upscaling law	Correlation Co-efficient R^2
Z_0-Evap-Fract (cm)	$Z0_{eff}=1.019\mu_{z0}-1.931*10^{-1}\sigma_{z0}-2.000*10^{-4}\sigma_{z0}^2+3.100*10^{-3}\mu_{z0}\sigma_{z0}-7.700*10^{-3}\sigma_{z0}^2$	*0.9985*
Z_0-SHF (cm)	$Z0_{eff}=1.018\mu_{z0}-2.372*10^{-1}\sigma_{z0}$	*0.9981*
Z_0-LHF (cm)	$Z0_{eff}=1.093\mu_{z0}-2.325*10^{-1}\sigma_{z0}-1.100*10^{-3}\mu_{z0}^2+7.200*10^{-3}\mu_{z0}\sigma_{z0}-1.360*10^{-2}\sigma_{z0}^2$	*0.9863*
Hs (g/kg)	$HS_{eff}=1.022\mu_{HS}-2.933*10^{-1}\sigma_{HS}-4.000*10^{-4}\mu_{HS}^2+7.500*10^{-3}\mu_{HS}\sigma_{HS}-1.660*10^{-2}\sigma_{HS}^2$	*0.9996*
Rcmin(sm^{-1})	$RCMIN_{eff}=1.029\mu_{RCMIN}-3.331*10^{-1}\sigma_{RCMIN}-1.000*10^{-4}\mu_{RCMIN}^2+1.200*10^{-3}\mu_{RCMIN}\sigma_{RCMIN}-2.400*10^{-3}\sigma_{RCMIN}^2$	*0.9997*
LAI (.)	$LAI_{eff}=1.029\mu_{LAI}-3.152*10^{-1}\sigma_{LAi}-4.100*10^{-3}\mu_{LAI}^2+5.790*10^{-2}\mu_{LAI}\sigma_{LAI}-1.252*10^{-1}\sigma_{LAI}^2$	*0.9993*
Rgl (Wm^{-1})	$RGL_{eff}=1.021\mu_{RGL}-2.064*10^{-1}\sigma_{RGL}-3.000*10^{-4}\mu_{RGL}^2+5.3*10^{-2}\mu_{RGL}\sigma_{RGL}-1.180*10^{-2}\sigma_{RGL}^2$	*0.9995*
Albedo (.)	$\alpha_{eff}=9.991*10^{-1}\mu_{\alpha}-4.150*10^{-2}\sigma_{\alpha}$	*0.9998*
Emissivity(.)	$\epsilon_{eff}=1.001*10^{-1}\mu_{\epsilon}-4.410*10^{-2}\sigma_{\epsilon}$	*0.9999*
Clapp-Horneberger b (.)	$b_{eff}=1.100\mu_b+1.462*10^{-1}\sigma_b-1.680*10^{-2}\mu_b^2-2.880*10^{-2}\sigma_b^2$	*0.9582*

b. Comparison with method of Hu et al.,(1999)

To assess the performance of our model, we use the scale invariance criteria of Hu et al. (1997) where the percentage difference or change of a grid model output with respect to aggregated output should be less than 10%. Fig.s 11 - 14 show the time series plot of percentage change for the sensible heat flux, latent heat flux, evaporative fraction and Bowen ratio respectively.

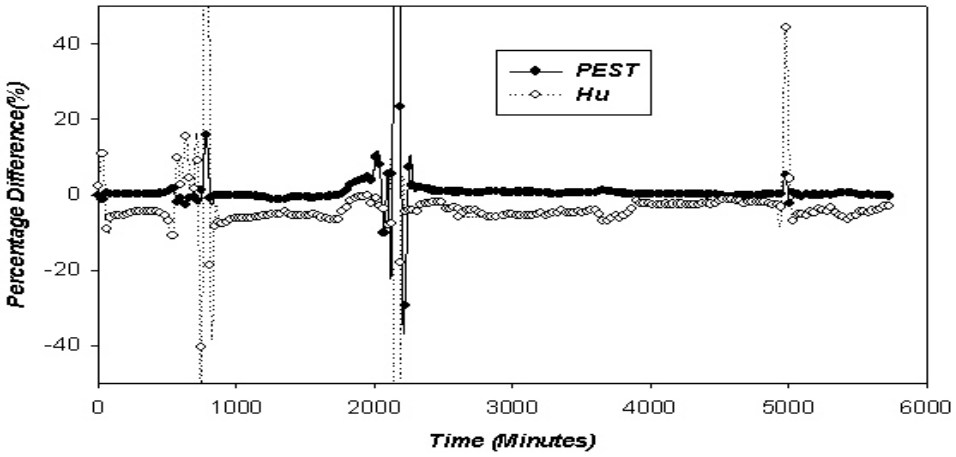

Fig. 11 : Percentage difference in sensible heat fluxes

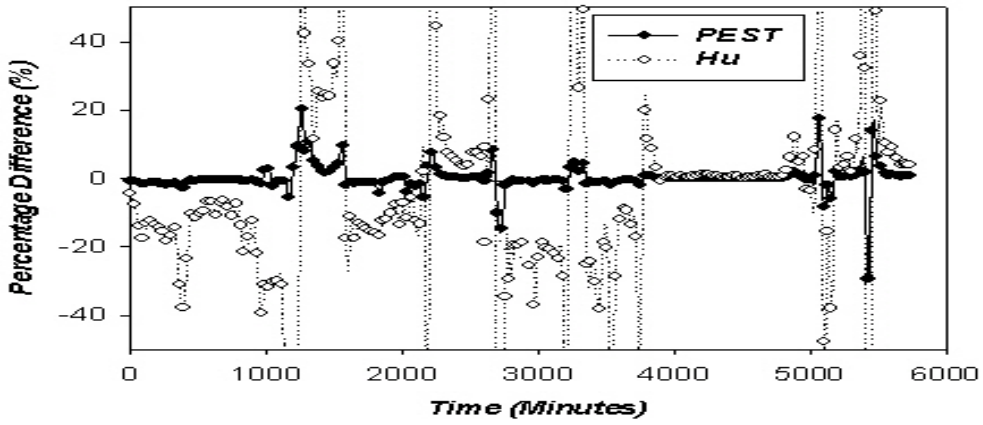

Fig. 12: Percentage difference in latent heat fluxes

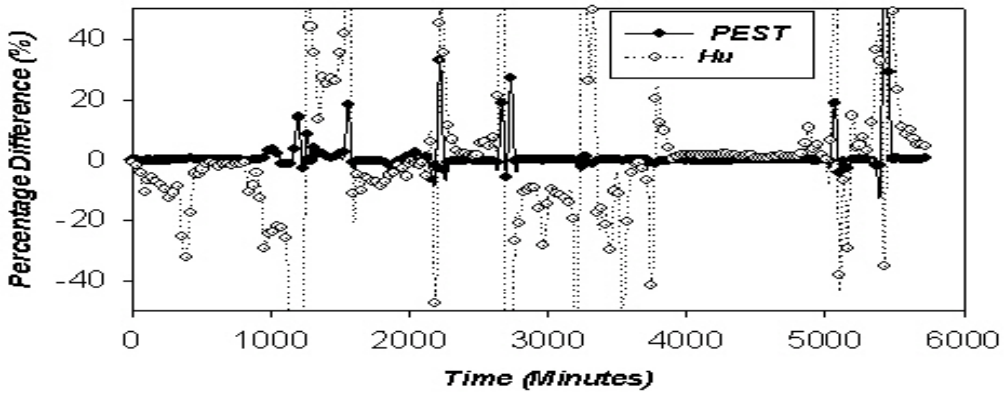

Fig. 13: Percentage difference in evaporative fraction

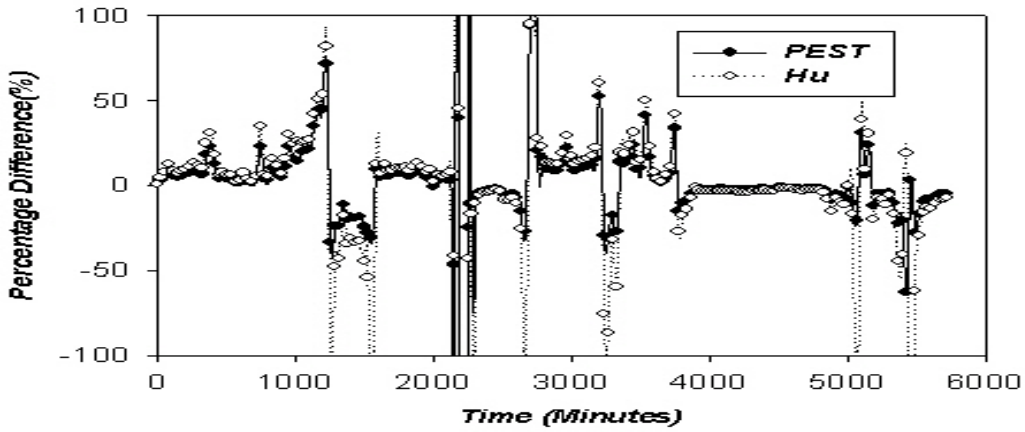

Fig. 14: Percentage difference in Bowen ratio

Although appreciable differences exist between values of effective roughness lengths for both methods at higher degrees of heterogeneity, the observed sensible heat fluxes were quite close. Methods of Hu et al (1999) overestimate the sensible heat flux where as our method consistently reduces the error to zero.

The latent heat flux show large percentage differences for method of Hu et al. (1999) where as our method consistently reduces it to zero. For our method, 7 out of 192 points violated the scale invariance criteria as against 112 out of 192 points for method of Hu et al. (1999). The evaporative fraction (Fig. 13) shows a similar trend to that of the latent heat flux (Fig. 12). For methods based on PEST, 7 out of 192 points violated the scale invariance condition as against 54 out 192 for that based on Hu et al. (1999). The Bowen ratio (ratio of sensible heat to latent heat) is inappropriate for scale invariance analysis because it is not well defined at vanishing latent heat fluxes as illustrated in

Fig. 14. Here, over 112 out of 192 points violated the scale invariant criteria for both methods.

3.3 Results for Coupled full Mesoscale Climate Model MM5-PEST: Surface energy fluxes and moisture indicators

a. Upscaling laws

Similarly, to account for sub-grid scale effects, we derived an upscaling law that maps the mean and standard deviation of the distributed land surface parameters at the sub-grid scale to their corresponding effective parameter at the grid scale for the coupled MM5-PEST case. Fig.s 15 - 19 show the respective plots of the upscaling law for surface emissivity, solar insolation factor, roughness length, surface albedo and minimal stomatal resistance. Table 4 gives the functional forms of these upscaling laws and the measure of goodness of fit. In the case of the surface emissivity and albedo, we found that a planar fit is best suited for interpolation between mean, standard deviation and effective values of emissivity and albedo.

We found that parabolic fits are best suited for interpolation between the mean, standard deviation and effective values of the solar insolation factor, roughness length and the minimum stomatal resistance. These results follow similar trend observed in the alone PEST-OSU runs.

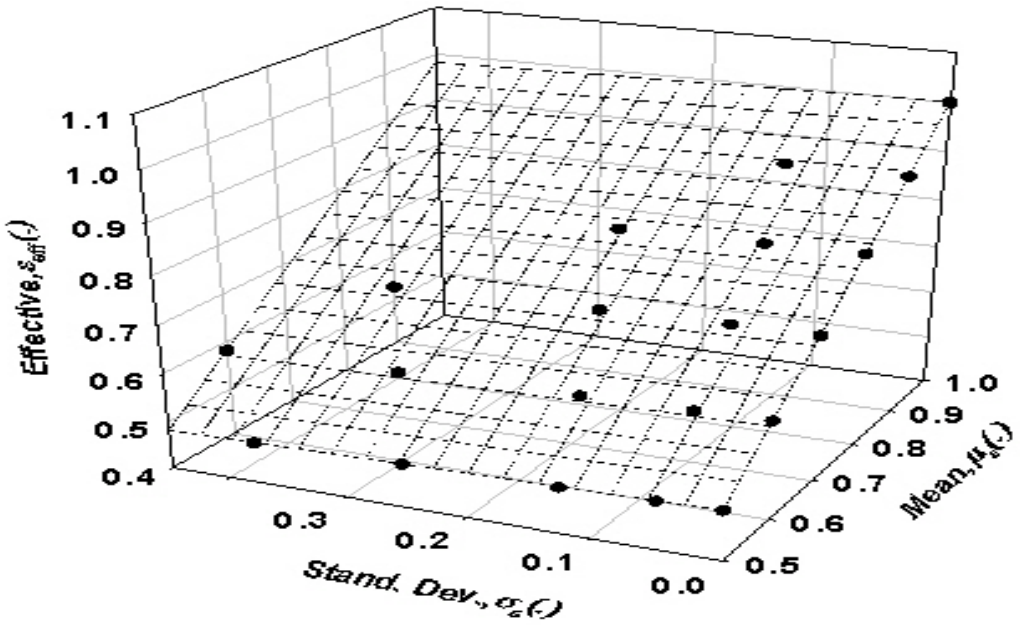

Fig. 15: Upscaling law for surface emissivity

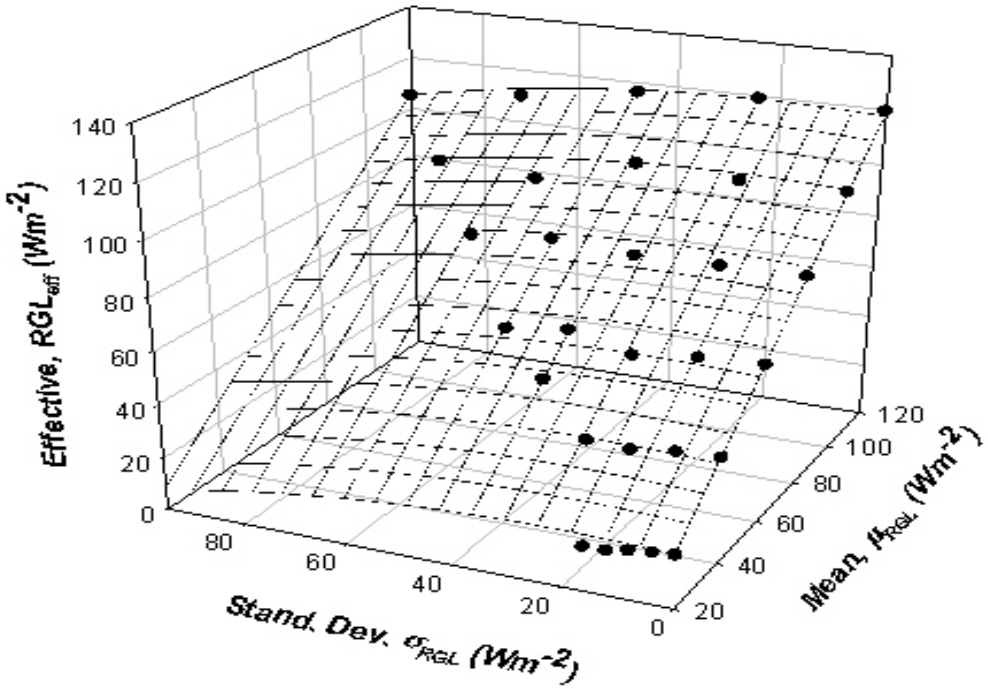

Fig. 16: Upscaling law for insolation parameter, Rgl

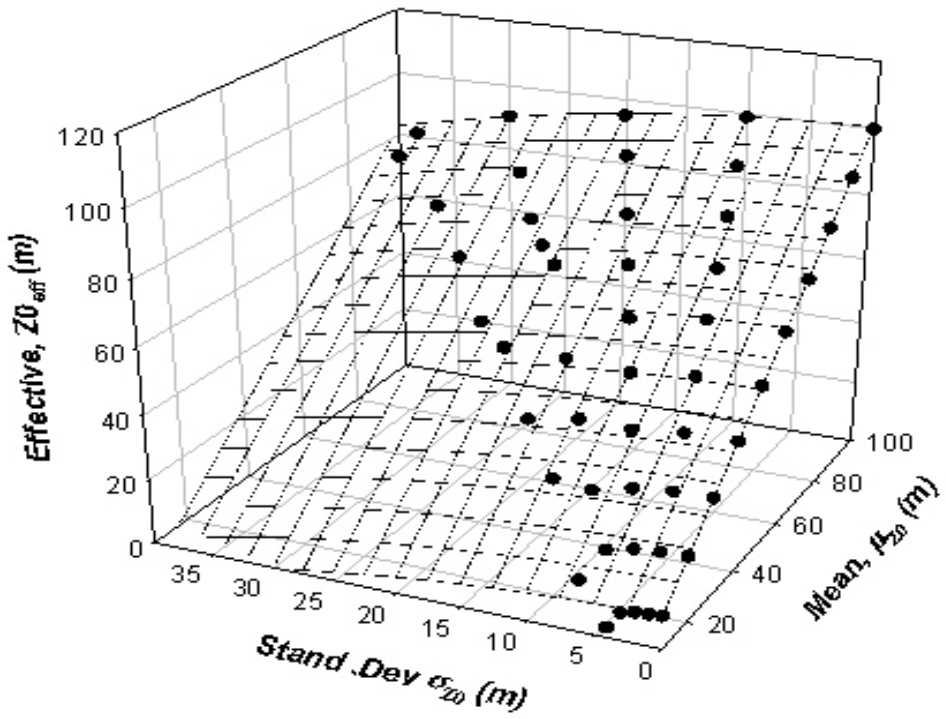

Fig. 17: Upscaling law for roughness length Z_0

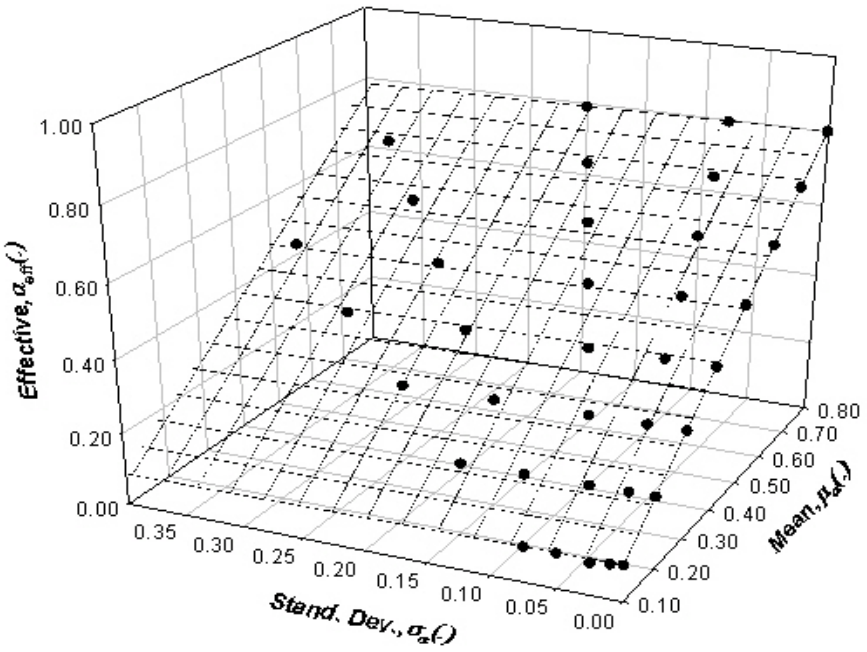

Fig. 18: Upscaling law for surface albedo α

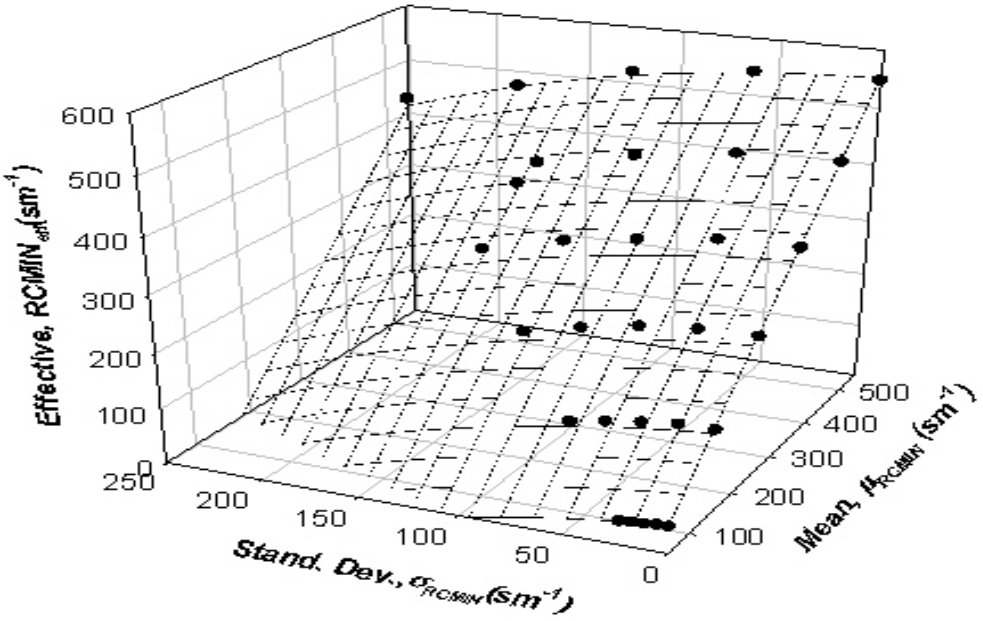

Fig. 19: Upscaling law for minimum stomatal resistance Rcmin

Table 2: UPSCALING LAWS: MM5-PEST

Parameter	Upscaling Law	Correlation Co-efficient R^2
Z_0-Evap-Fract (cm)	$Z0_{eff}=1.095\mu_{z0}-1.092\sigma_{z0}-1.200*10^{-3}\mu_{z0}^2+1.480*10^{-2}\mu_{z0}\sigma_{z0}-1.530*\sigma_{z0}^2$	*0.9761*
Rcmin (sm^{-1})	$RCMIN_{eff}=1.019\mu_{z0}-3.752*10^{-1}\sigma_{z0}-3.001\mu_{z0}^2+6.000*10^{-4}\mu_{z0}\sigma_{z0}-2.000*10^{-3}\sigma_{z0}^2$	*0.9986*
Rgl (Wm^{-2})	$RGL_{eff}=9.397*10^{-1}\mu_{RGL}+1.649*10^{-1}\sigma_{RGL}+6.000*10^{-4}\mu_{RGL}^2-2.400*10^{-3}\mu_{RGL}\sigma_{RGL}-3.000*10^{-4}\sigma_{RGL}^2$	*0.9871*
Albedo (.)	$\alpha_{eff}=9.991*10^{-1}\mu_{\alpha}-4.150*10^{-2}\sigma_{\alpha}$	*0.9998*
Emissivity (.)	$\epsilon_{eff}=1.001*10^{-1}\mu_{\epsilon}-4.410*10^{-2}\sigma_{\epsilon}$	*0.9999*

b. Comparison with method of Hu et al. (1999)

For the coupled MM5-PEST runs, the results generally show similar trends to that of the SVAT-PEST runs. However, marked differences exist for the sensible heat flux where the relative changes during night time violates the scale invariance criteria due to sign changes and very low values of the sensible heat fluxes as illustrated in Figs. 20 and 21. Careful examination of the plots show that generally both methods perform very well as the residual fluxes at night time are insignificant (almost zero) to affect the energy dynamics appreciably.

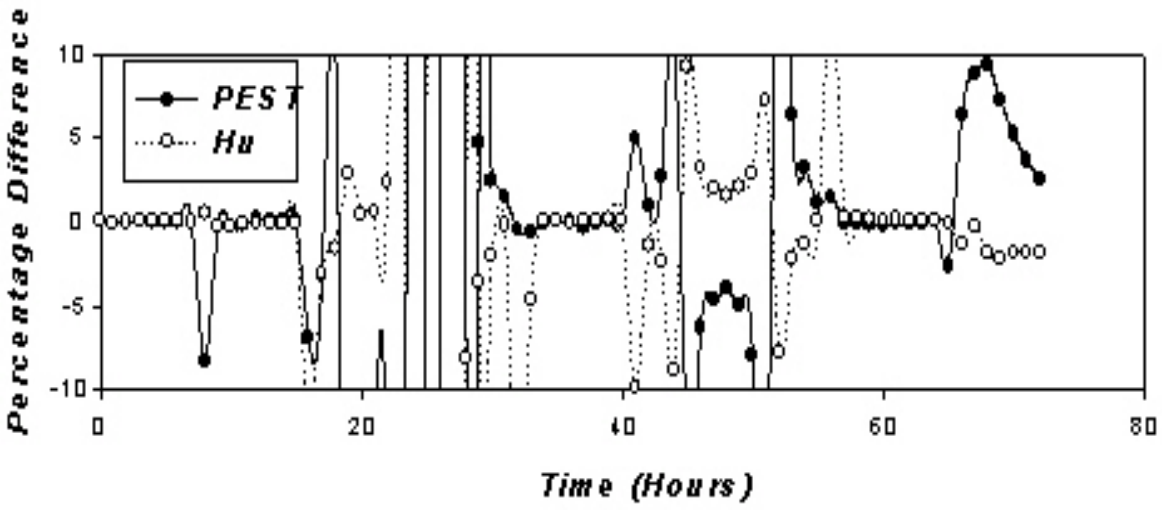

Fig. 20: Percentage difference in sensible heat fluxes

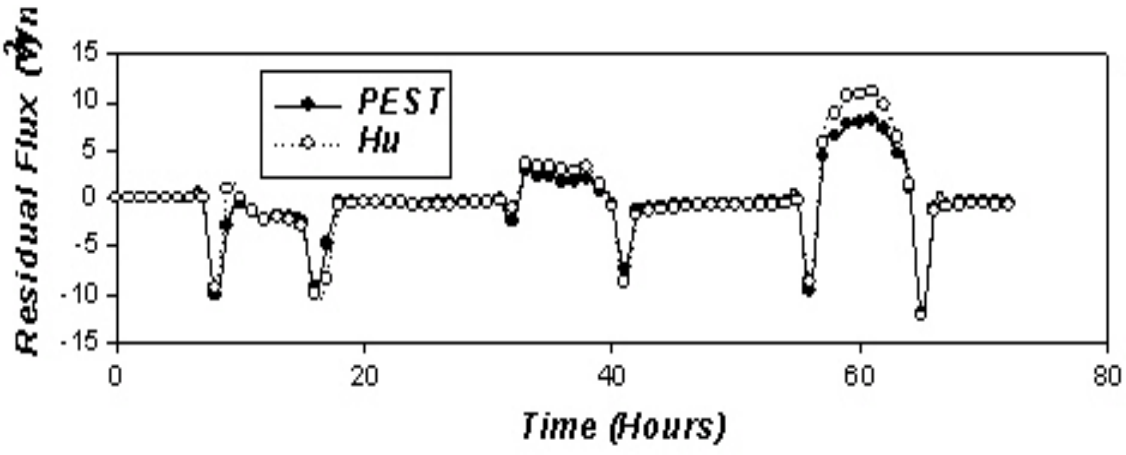

Fig. 21: Residual sensible heat fluxes

Figs. **22** and **23** give the respective percentage difference plots for latent heat fluxes and evaporative fraction. For the latent heat fluxes and evaporative fraction both

methods satisfy the scale invariance condition very well, while our method is performing even much better than Hu et al. (1999).

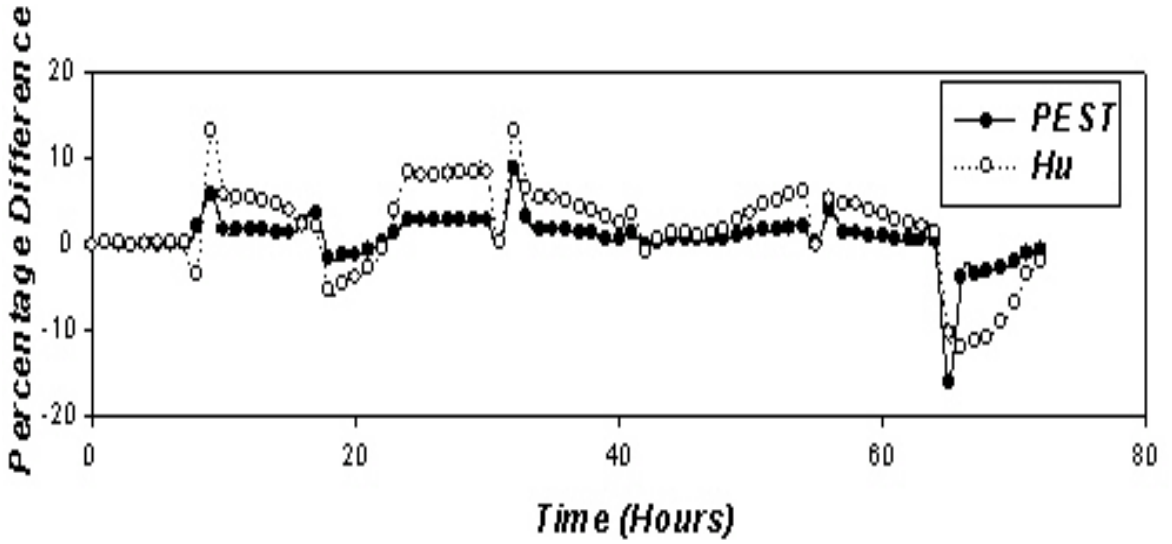

Fig. 22: Percentage difference in latent heat fluxes

This suggests that the lateral interactions between adjacent cells tend to minimize the observed errors quite well than in the stand-alone version (SVAT) where these interactions are assumed negligible.

For lower degrees of sub-grid scale variability, the two methods give the same parameter estimates for roughness length.

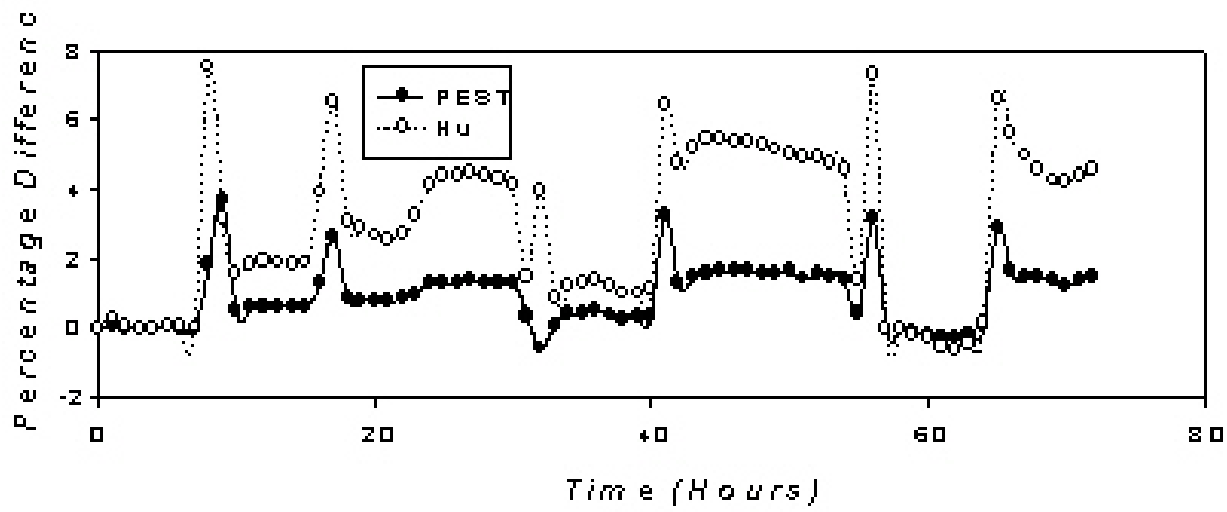

Fig. 23: Percentage difference in evaporative fraction

For the derivation of effective albedo, reflected shortwave radiation is used as objective function. In case of emissivity, surface temperature is applied. Here, Hu et al. (1999) and our method yield nearly identical results (Figs. 24 and 25 respectively). The associated errors are negligible confirming results from related works (Hu et al, 1997, 1999 and Li et al.,1994).

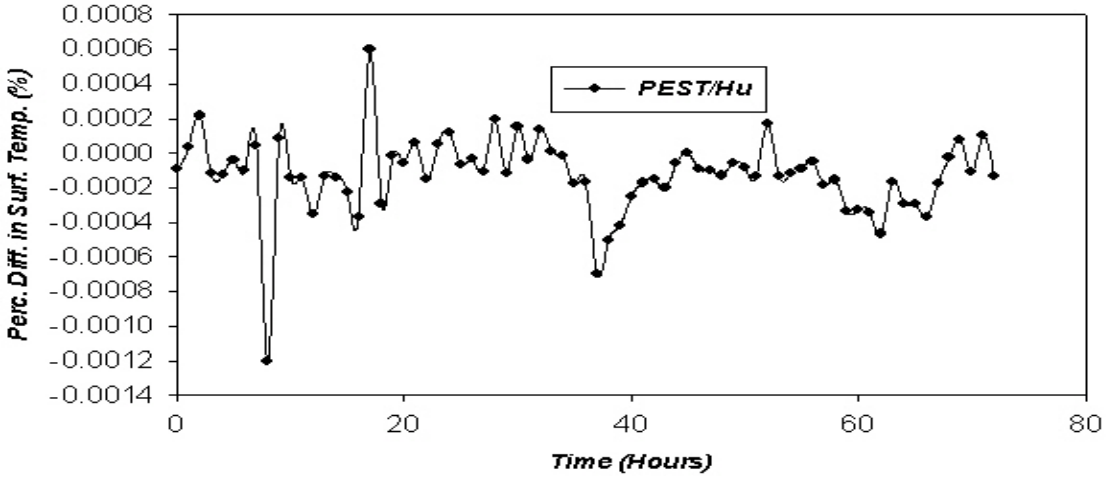

Fig. 24: Plot of percentage difference in surface temperature

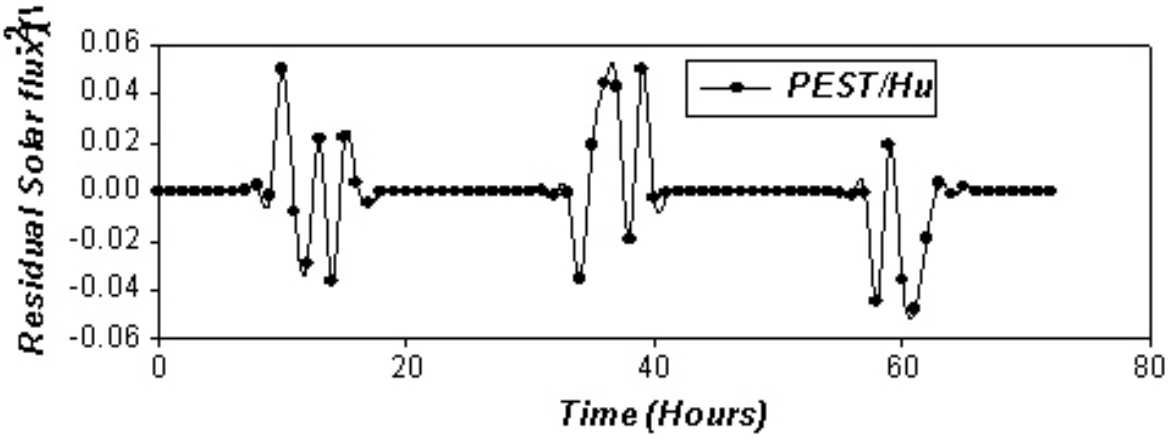

Fig. 25: Plot of residual solar flux

c. Effects of fitting functions, initial parameters and parameter bounds on results of the parameter estimation process.

An important component of the research was to find effective ways of saving computer resources during the parameter estimation process by reducing the duration of model

runs while ensuring accurate results. The main requirements for achieving a feasible solution and faster convergence to the true solution are 1) the initial parameter set must lie within the region R, bounded by the parameter set containing the global minimum, 2) the fitting function must be continuously differentiable for the range of parameters bounded by the region R and 3) the covariance matrix for the parameters bounded by the region R must be nonsingular and continuous function for the range of parameters bounded by the region R (Cooley et al.,1990).

To realise these objectives, transformation of the functions of interest (latent and sensible heat fluxes) to a form (e.g. like evaporative fraction) that guarantees a feasible solution and faster convergence was made. Similarly, much effort was made to obtain good initial parameters that are within the close neighbourhood of the true solution (condition 1 above) using limiting cases of the transformed functions and other well-known methods (Hu et al.,1999;Noilhan et al.,1996 and Altaf et al.,1996). Additionally, a criterion for parameter bounds was developed to restrain the solution from wandering in the non-feasible region of the parameter search space and hence saving computing resources and CPU time. The lower and upper bounds were respectively obtained as the harmonic and arithmetic means of the subgrid scale parameters.

Most of the results obtained in this experiment are closer to the geometric mean of the subgrid scale parameters, GM, which is also bounded by the harmonic and arithmetic means. This is similar to what was observed in the stand-alone mode of the PEST-OSU runs.

Verification and implementation of the above assumptions were made by undertaking model runs for fitting functions of evaporative fraction, latent and sensible heat fluxes using the same initial parameter of 31.8cm obtained by method of Hu et al.(1999). We then fed the results for each fitting function to MM5 and compared the results to the aggregated sensible heat fluxes (observation). Model calls for evaporative fraction, latent and sensible heat fluxes were 26, 20 and 45 and parameter estimates 72.42cm, 42.84cm and 69.99cm respectively. Although the model calls for sensible heat flux is the least, it has the poorest fit as it is trapped in a local minimum. Evaporative fraction has the best fit and second least model calls. These results are given in table 3 and illustrated in figs. 26 and 27.

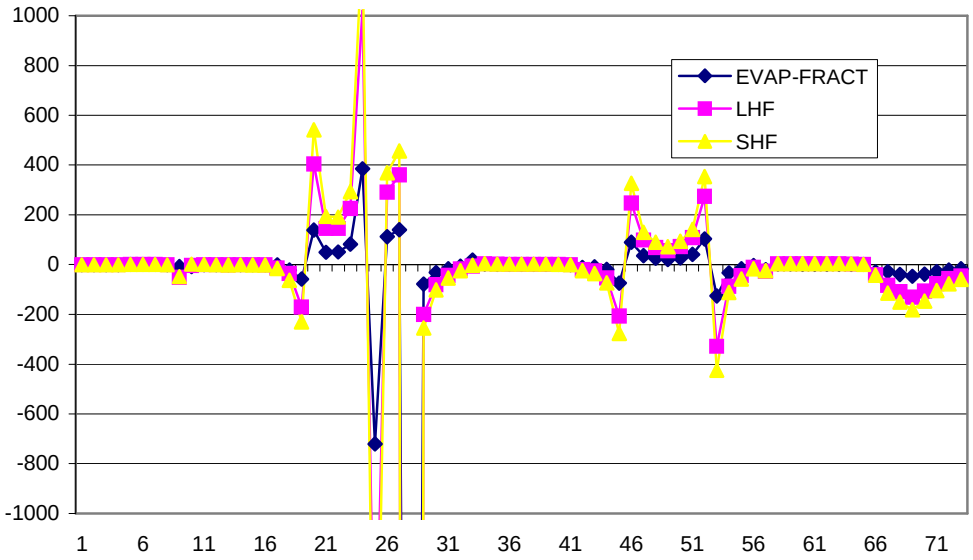

Fig. 26: Sensible heat fluxes based on Z_0 estimates for different fitting functions.

Table 3: Comparison of fitting functions

Fitting function	**Number of model calls**	**Roughness length (cm)**
Evaporative Fraction (.)	*26*	*72.72*
Latent Heat Flux (Wm^{-2})	*45*	*69.99*
Sensible Heat Flux (Wm^{-2})	*20*	*42.84*

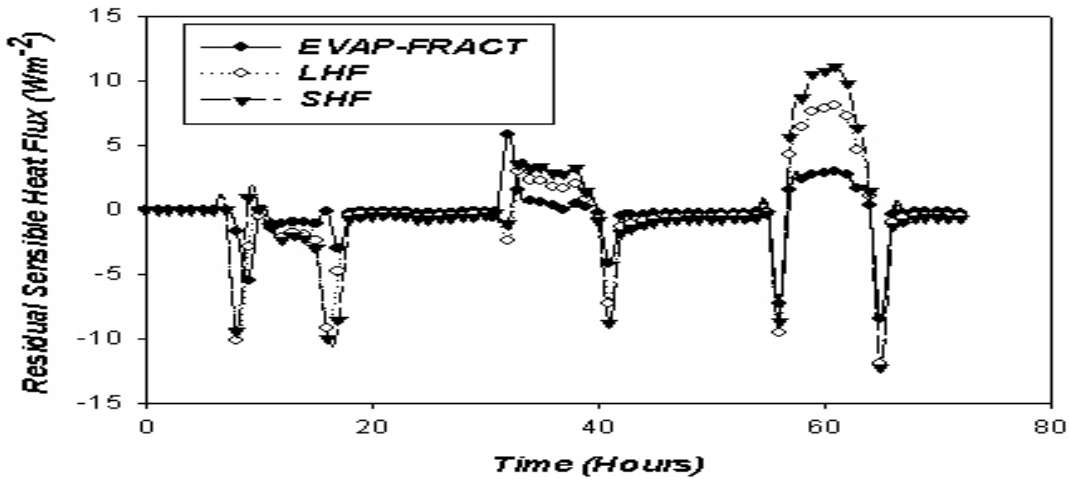

Fig. 27: Residual sensible heat fluxes based on Z0 estimates for different fitting functions.

We further investigated the effect of our choice of initial parameters on the result of the parameter estimation process. We chose initial values based on the mean, Hu et al. (1999) and an arbitrary value of half the mean. The results show that parameter estimates obtained using initial values of Hu et al. (1999) gives the best results as shown in fig. 28.

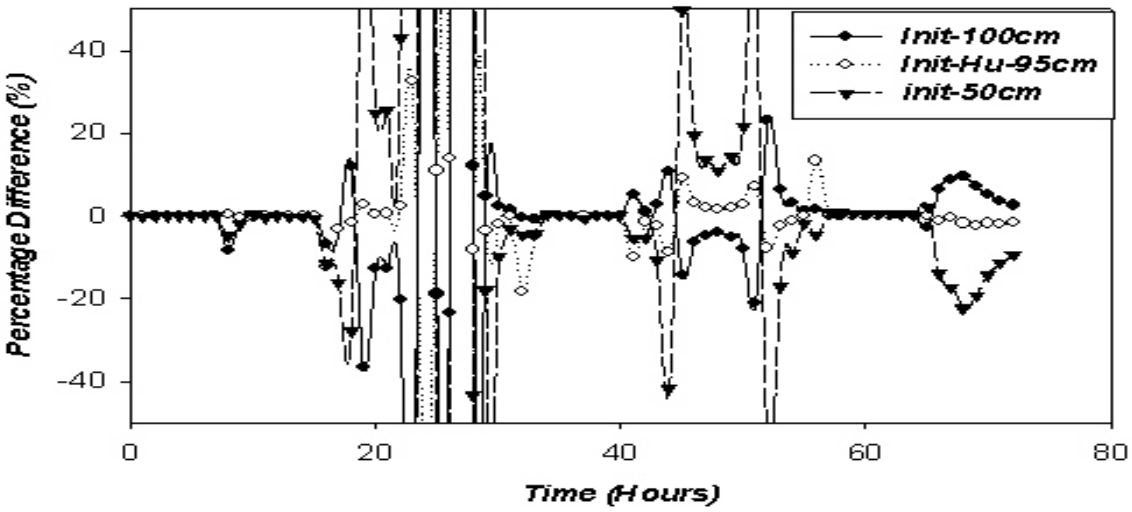

Fig. 28: Sensible heat fluxes based on different initial Z0 estimates.

Transformation of fitting functions from sensible and latent heat to evaporative fraction gave the following advantages:

- Better measures of fit
- Reduced total number of model calls leading to reduction in simulation time per parameter estimation process. On the average over a 100% reduction in simulation time was realized. This translates on the average from about 2-3 days to 1 day per parameter estimation process.
- Improved/more accurate estimates
- Savings in computer resources

The main benefit was that upscaling laws that require over 60 parameters could be obtained within 2-3 weeks instead of about three months observed in previous experiments.

Exploration of Parameter Space – Identification of Indeterminate States and Qualified Initial Guesses

To undertake the parameter estimation process, PEST must be initialized with good initial parameter estimates so as to increase the chances of locating the optimal parameter set. For this reason we look for approximate aggregation schemes based on physics compatible with that of the OSU-LSM. To justify our choice of initial parameter estimates and also validate the performance our proposed scheme, we used PEST's PARREP facility (Doherty, 2000) and OSU-LSM to produce chi square values for some selected parameter values that scan the parameter spaces of the land surface parameters of interest. We then developed plots of chi squared versus land surface parameters and compared the results with the methods outlined above and our proposed method.

The chi squared plots for the various effective land surface parameters are given in Fig. 31 to Fig. 32. (with the legend in fig.34).

These results show that our choice of initial parameter estimates is justified as the initial parameter sets lie within reasonable ranges (neighbourhood) of the chi squared minima. It was observed that a criteria for the parameter bounds can be defined

$$HM \leq p_{eff} \leq AM \tag{3}$$

where HM and AM are respectively the harmonic and arithmetic means of the subgrid scale parameters. The arithmetic, harmonic and geometric means are defined by

$$AM = \frac{1}{n} \sum_{i=1}^{n} p_i \tag{4}$$

$$HM = \frac{1}{n} \sum_{i=1}^{n} \frac{1}{p_i} \tag{5}$$

$$GM = \left(\prod_{i=1}^{n} p_i \right)^{\frac{1}{n}} \tag{6}$$

where n is the number of subgrid scale parameters.

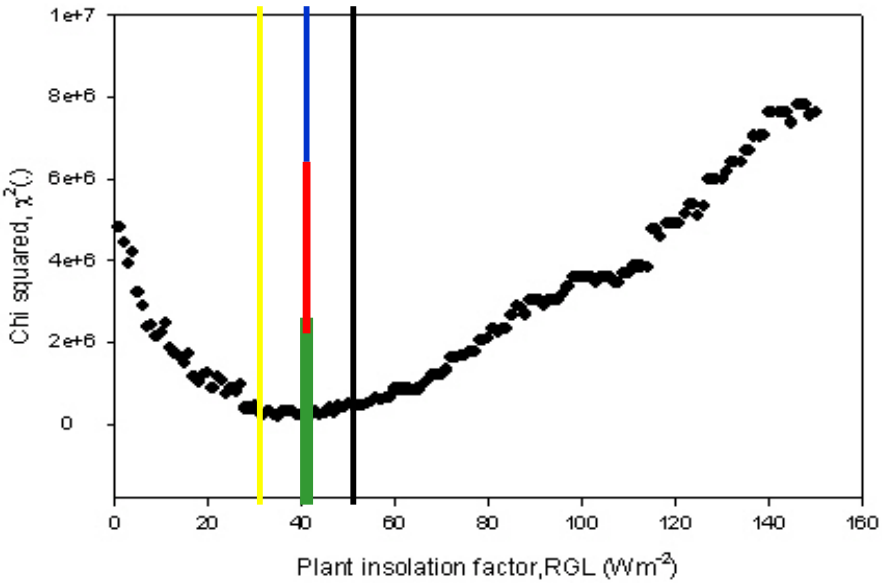

Fig. 29: Chi square plot for plant insolation factor Rgl

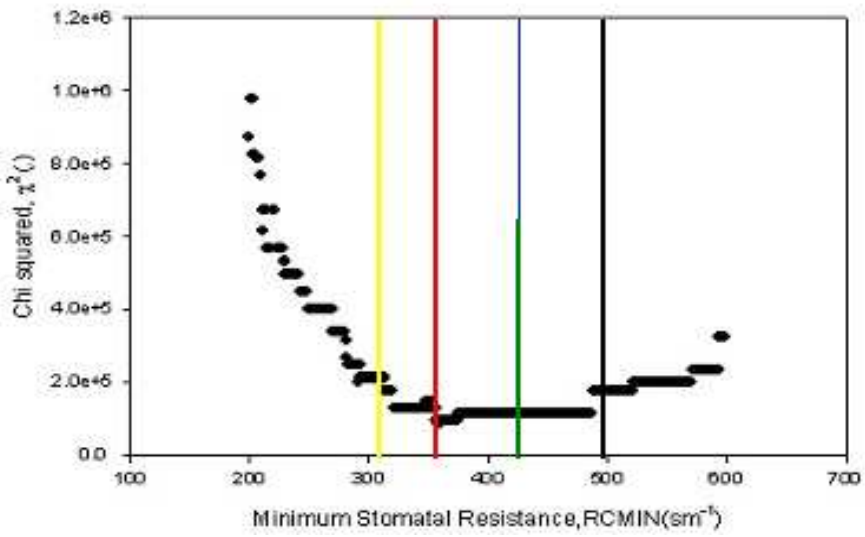

Fig. 30: Chi square plot for minimum stomatal resistance, Rcmin

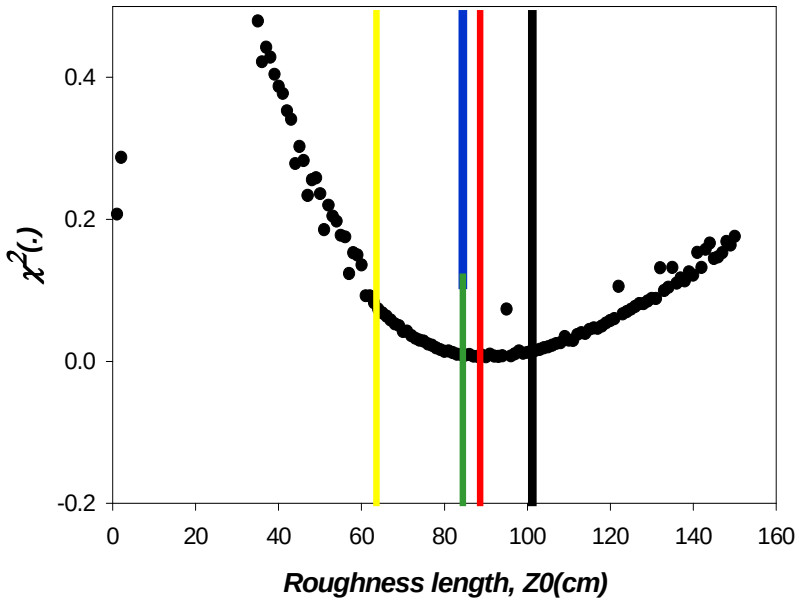

Fig. 31: Chi squared plot for roughness length, Z_0

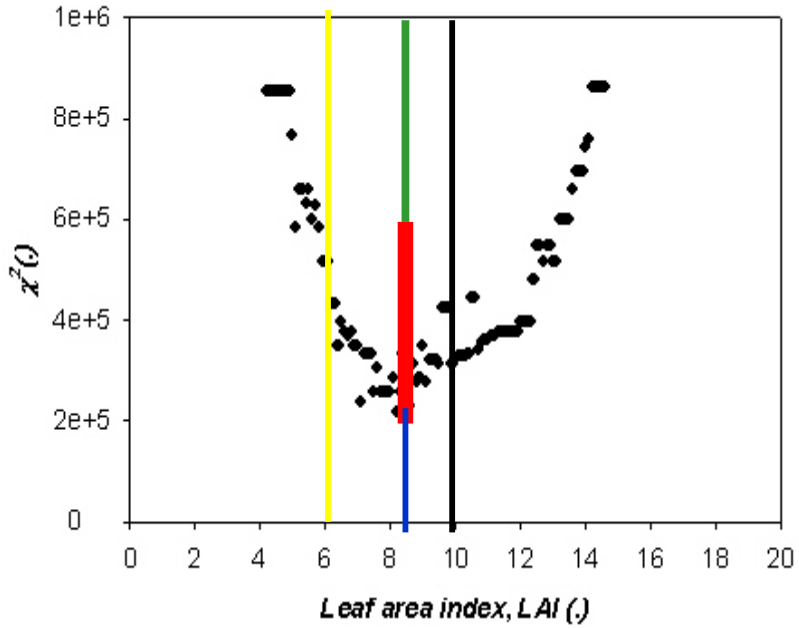

Fig. 32: Chi square plot for leaf area index, LAI

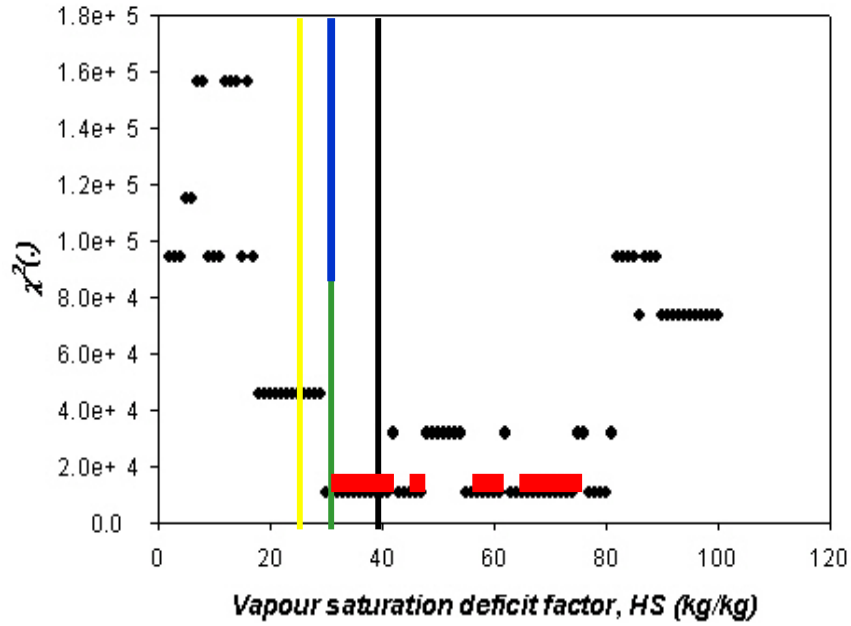

Fig. 33: Chi square plot for vapor pressure deficit factor Hs

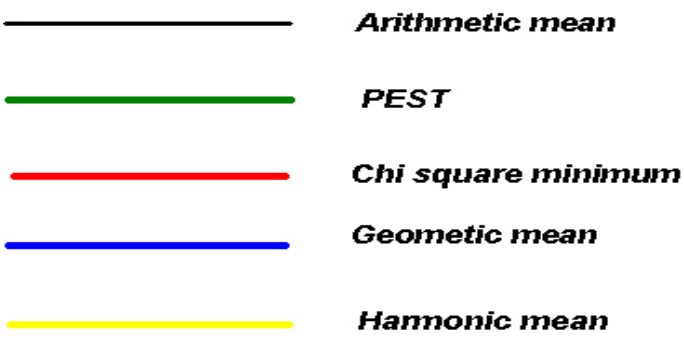

Fig. 34: Legend for Chi square analysis plots

The chi square analysis reveals points of sudden jumps, whose origin is not yet understood. Numerical instabilities might be a reason for it or simply erroneous programming of underlying physical equations. The parameter estimation process has difficulties in locating the chi square minimum along the chi square gradient, leading to indeterminate solutions in case of LAI, Hs and Rcmin. Here, a qualified good guess (i.e. close to the effective parameter) for the initial parameter is essential for the success of the inverse modeling.

We also observed that the optimal parameter sets are very close to the geometric means of the distributed land surface parameters. The method of Hu etal.,(1999) is based on the harmonic mean of the distributed land surface parameters. In this scheme, corrections for errors associated with the approximations made in formulating the scheme are difficult to quantify and hence it tends to underestimate the roughness length. The geometric mean, which is an upper bound for the harmonic mean seems to capture these errors quite well. Similar arguments can be made for the method of Noilhan et al. (1996) whose parameter estimates for minimum stomatal resistance is based on the harmonic mean. The aggregation scheme proposed by Noilhan et al. (1996) for estimating effective leaf area index which is based on the arithmetic mean over estimates the leaf area index. The geometric mean, which is a lower bound to the arithmetic mean approximates the optimal parameter set very well.

The conclusion drawn from these results is that the geometric mean is an important aggregation scheme for aggregating land surface parameters and hence surface energy fluxes.

To check the uniqueness of the parameter estimation process for the duration of runs, the estimation process was done for roughness length for a period of four days and thirty days respectively using the coupled SVAT-PEST model. The roughness length

obtained for the four and thirty days were respectively 69.88cm and 70.90cm. This shows uniqueness of the parameter estimation process with respect to duration of forcing data as shown in fig. 34.

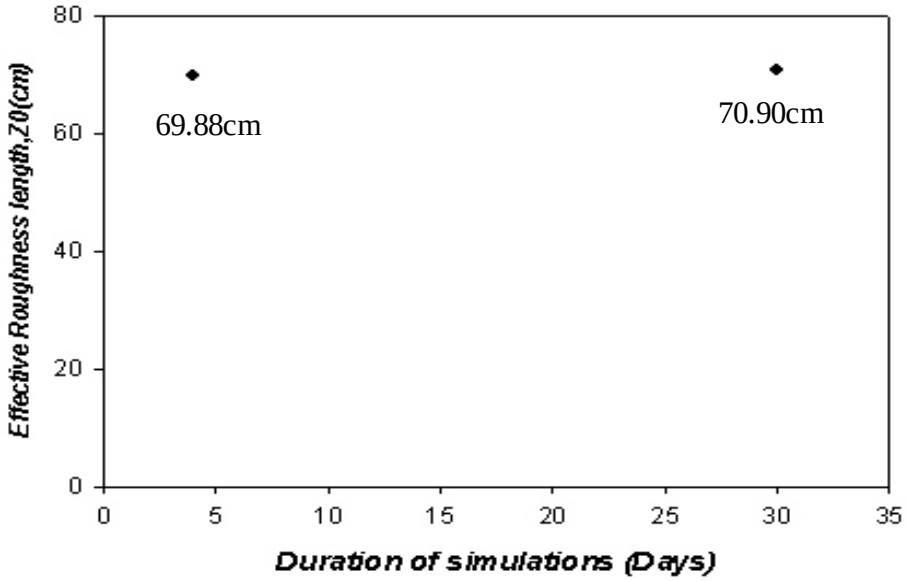

Fig. 34: Effective parameters derived are independent of meteorological forcing within the time scale days-month.

4.0 GENERAL DISCUSSION AND CONCLUSION

4.1 Method

We have shown how inverse modelling can be used to obtain effective parameters and established scale invariance for the surface energy fluxes (latent and sensible heat fluxes), moisture indicators (Bowen ratio and evaporative fraction), surface temperature, and reflected shortwave radiation.

To justify our choice of initial parameter estimates and also validate the performance our proposed scheme, we used PEST's PARREP facility (Doherty, 2000) and OSU-LSM to produce chi squared values for some selected parameter values that scan the parameter spaces of the land surface parameters of interest. We then developed plots of chi squared versus land surface parameters and compared the results with the methods outlined above and our proposed method. The results show that our method

performs very well and also the methods we used for estimating the initial parameters are appropriate.

We have also shown the limitations involved in implementing inverse modelling when the function of interest is not well defined as illustrated in the example on the Bowen ratio. Information obtained from these plots enables one to develop better strategies for analyzing residual errors to improve the parameter estimation process. For example, we know from this study that in the stand alone coupled SVAT-PEST runs, the residual error distribution for parameter estimates based on Hu et al. (1999) is Gaussian for latent heat fluxes and evaporative fraction, hence we can use the relevant parameter transformation to improve the parameter estimates. Similarly, an appropriate parameter transformation can be made in the case of the sensible heat flux estimates based on Hu et al. (1999) which consistently overestimates the observed sensible heat fluxes.

On the other hand, the plots for the evaporative fraction are well within the scale invariant condition for both methods in the coupled MM5-PEST runs. This is due to the fact that the evaporative fraction is well defined (bounded between 0 and 1) and stable. This is a requirement for parameter convergence and hence makes the evaporative fraction a natural choice for the parameter estimation formulation for roughness length. As there exist a strong mutual dependence of the latent and sensible heat fluxes on roughness length, using evaporative fraction as model output response in estimating the roughness length captures parameter sensitivities that properly reflect their interdependencies.

A criterion for determining effective parameter bounds was developed to restrain the search process from wandering in the non-feasible region of the parameter space and hence reducing model run time considerably. The lower and upper limits of the effective parameter bounds were found to be the harmonic and arithmetic means of the subgrid scale parameters respectively.

Moreover, it is important to note that our method provides effective parameters that are independent of the length of the forcing episode; in case of other methods (Chehbouni et al., 1995) this is not the case; Hu et al. (1999) require an approximation on the temperature difference between subgrid and grid to achieve this goal.

4.2 Results

Summary of the results of the upscaling laws for the landsurface parameters are given in tables 4 and 5 below.

Table 4: Coupled MM5-PEST Parameter Upscaling Laws and Objective Functions

Parameter	**Objective function**	**Upscaling law**	**Comparison**
Roughness length Z_0	Evaporative Fraction	Parabolic	Under estimation of Z_0 by Hu et al.(1999)
Minimum stomatal resistance Rcmin	Evaporative Fraction	Parabolic	Under estimation of Rcmin by Noilhan(1996)
Insolation factor Rgl	Evaporative Fraction	Parabolic	Under estimation of RGL by Noilhan (1996)
Surface emissivity ε	Surface Temperature	Planar	Same as PEST
Surface albedo α	Reflected Shortwave	Planar	Same as PEST

Table 5: Coupled SVAT-PEST Parameter Upscaling Laws and Objective Functions

Parameter	**Objective function**	**Upscaling law**	**Comparison**
Roughness length Z_0	Evaporative Fraction	Planar or weak Parabolic	Under estimation of Z0 by Hu et al.(1999)
Minimum stomatal resistance Rcmin	Evaporative Fraction	Parabolic	Under estimation of Rcmin by Noilhan (1996)
Insolation factor Rgl	Transpiration	Parabolic	N/A
Leaf area index LAI	Transpiration	Parabolic	Over estimation of LAI by Noilhan (1996)
Vapour pressure deficit factor Hs	Transpiration	Parabolic	N/A
Surface emissivity ε	Surface Temperature	Planar	Same as PEST
Surface Albedo α	Reflected Shortwave	Planar	Same as PEST
Clapp-Hornberger parameter b	Soil evaporation	Parabolic	N/A

In conclusion, our method provides a convenient framework for upscaling land-surface parameters such that surface energy fluxes and moisture indicators in complex terrains become scale invariant. To extend the applicability of our method, we undertook an investigation of its implementation in a full mesoscale climate model (MM5) to account for the lateral interactions between atmospheric state variables and soil moisture of adjacent grids and the result was very promising. It was seen that the overall upscaling laws (planar, parabolic) themselves do not differ between the full 3-D version and the stand alone version. However, the parameters appearing in the regression function differ: in general, the curvature show higher slopes in the fully 3-D mode.

4.3 Outlook

Outlook for future work would include the implementation of the derived scaling laws in a mesoscale meteorological model to account for subgrid scale effects of the heat fluxes and apply it for regional climate simulations. In particular, the influence of cluster effects in subgrid-scale variability must be investigated. Extended runs are also needed to investigate the influence of seasonal variability of land surface parameters on scale invariance and how to properly represent spatio-temporal variability of landsurface processes at such scales.

5.0 REFERENCES

ALTAF M. A., MICHAUD J., SHUTTLEWORTH W. J., AND DOLMAN A. J. (1996): Testing of Vegetation Parameter Aggregation Rules Applicable to the Biosphere-Atmosphere Transfer Scheme (BATS) and the FIFE site, Journal of Hydrology. **177**, 1-22.

CHEHBOUNI, A., NJOKU, E.G., LHOME, J.P. AND KERR, Y.H. (1995): Approaches for averaging surface parameters and fluxes over heterogeneous terrain, J. Climate **8**, 1386 - 1393

COOLEY, R.L. AND NAFF, R.C.(1990): Regression Modelling of Groundwater Flow, USGS Publication in Hydraulic Modelling **3**, 70 –71.

DOHERTY, J. (2002): PEST – Model-Independent Parameter Estimation, Watermark Numerical Computing, Australia.

EK., M., MAHRT, L. (1991): OSU 1-D PBL Model User's Guide, Version 1.0.4, Oregon State University, Department of Atmospheric Sciences, USA.

HU Z., AND ISLAM S. (1997): Effects of Spatial Variability on the scaling of Land Surface Parametrisations, Boundary Layer Meteorology. **83**, 441-461.

HU Z., AND ISLAM S. (1999): Approaches for Aggregating Heterogeneous Surface Parameters and Fluxes from Mesoscale and Climate Models, Boundary Layer Meteorology. **24**, 312-336.

LI, B. AND AVISSAR, R. (1994): The Impact of Spatial Variability of Land-Surface Characteristics on Land-Surface Heat Fluxes, J. Climate **7**, 527-537.

MEYERS, T.P., AND EK, M. (1999): NOAH-LSM User's Guide version 2.2, ftp://ftp.ncep.noaa.gov/pub/gcp/ldas/noahlsm/ver_2.2

NOILHAN, J. AND MAHFOUF J.F. (1996): The ISBA land surface parameterisation scheme, Global and Planetary Change **7,** 145 – 159.

LIST OF SYMBOLS

Symbol	Meaning
Rcmin	Minimum Stomatal Resistance
Hs	Vapor pressure deficit function
Rgl	Solar insolation factor
Z_0	Roughness length
LAI	Leaf Area Index
p	Land surface parameter
z	Vertical distance
b	Clapp-Hornberger soil parameter
p_{eff}	Effective parameter of land surface property
LHF	Latent heat fluxes
SHF	Sensible heat fluxes
EVAP-FRACT	Evaporative fraction
Trans	Transpiration rate
G	State variable
f	function
g	Random number generator
a_i	fractional cover of the i-th subgrid
σ_p	Standard deviation of a given distributed land surface parameter
μ_p	Mean of a given distributed land surface parameter
α	Surface Albedo
ε	Surface emissivity
χ^2	Objective function, Mean of the Square Error or Chi square value
HM	Harmonic Mean
GM	Geometric Mean
AM	Arithmetic Mean
PD	Percentage Difference
F_c	Observed fluxes
F_e	Simulated fluxes
i,j	Indices

Definitions

Scale invariance: A map or function is said to be scale invariant if:

- The parameters of the map are homogeneous over the grid
- The map is a linear combination of inputs and parameters

Quasi-scale invariance: If the error or percentage difference between the aggregated output from a distributed map and that from the lumped map is less than 10%.